Available online at www.sciencedirect.com
ScienceDirect
Journal of Power Sources 179 (2008) 395–400
JOURNAL OF POWER SOURCES
www.elsevier.com/locate/jpowsour

Short communication

Electrochemical performance of ZnO nanoplates as anode materials for Ni/Zn secondary batteries

M. Ma [a], J.P. Tu [a,*], Y.F. Yuan [b], X.L. Wang [a], K.F. Li [a], F. Mao [a], Z.Y. Zeng [a]

[a] *Department of Materials Science and Engineering, Zhejiang University, Hangzhou 310027, China*
[b] *School of Mechanical and Automation Control, Zhejiang Sci-Tech University, Hangzhou 310032, China*

Received 12 October 2007; received in revised form 30 December 2007; accepted 4 January 2008
Available online 20 January 2008

Abstract

Plate-like ZnO with good crystallinity were prepared by a simple hydrothermal synthesis method in $Zn(NO_3)_2{\cdot}6H_2O$ and NaOH solution at 180 °C. The dimension of ZnO powder ranged from 200 to 500 nm and the average thickness was about 50 nm. The electrochemical performances of ZnO nanoplates as anode active materials for Ni/Zn cells were investigated by galvanostatic charge/discharge cycling and cyclic voltammogram (CV). The ZnO nanoplates showed better cycle stability than the conventional ZnO, and the discharge capacity maintained 420 mAh g^{-1} throughout 80 cycling tests. At the same time, they also exhibited higher midpoint discharge voltage and lower midpoint charge voltage. The continual SEM examinations on the electrode found that the morphology of the plate-like ZnO active material did not change essentially and the zinc dendrite was suppressed effectively, which resulted in the improvement of cycle stability of Ni/Zn secondary cells.

Keywords: ZnO nanoplates; Electrochemical performance; Cycling stability; Nickel zinc secondary battery

1. Introduction

Ni/Zn secondary battery has advantages of high specific energy, high specific power, high open-circuit voltage, low toxicity and low cost. However, the widespread commercialization of this kind of Zn-based battery is limited due to its low cycling life. The major problems in rechargeable Ni/Zn batteries are the shape change of electrode, dendrite growth, passivation and self-discharge of the Zn electrodes [1–3]. Many attempts have been made to overcome these problems, including additives to the zinc electrode [4–8] or the electrolytes [9–11]; selection of stable separators [12,13]. Other techniques such as pulse charging, intermittent charging and electrode vibration have been applied.

It is well known that these problems of Ni/Zn secondary batteries are tightly related to physical and electrochemical properties of ZnO. Therefore, the investigations and treatments on ZnO are very important approaches to improve the electrochemical performance of Ni/Zn batteries. The initial morphology of ZnO was found to be able to influence the electrochemical performance of secondary Zn batteries, for example, prismatic ZnO and ZnO nanorods as anode active materials could improve the lifetimes of the zinc electrode [14]. Our previous work already indicated that plate-like ZnO was an important intermediate product and influencing factor during the charging/discharging process of ZnO [15]. In this present work, nanosized ZnO with plate-like morphology was prepared by the hydrothermal method. The electrochemical properties of ZnO nanoplates as the anodic active materials for Zn/Ni cells were in detail investigated.

2. Experimental

2.1. Preparation of ZnO nanoplates

Nanosized plate-like ZnO was prepared by a simple hydrothermal synthesis method [16]. 0.05 mol NaOH and 0.005 mol $Zn(NO_3)_2{\cdot}6H_2O$ were dissolved into 80 ml distilled water under magnetic stirring, and then white precipitation was obtained. Subsequently, the precipitation was transferred into a cylindrical Teflon-lined stainless steel autoclave with a capacity of 140 ml, and the autoclave was sealed and kept in a furnace at 180 °C for 5 h. After cooling, the product was collected from the

* Corresponding author. Tel.: +86 571 87952573; fax: +86 571 87952856.
E-mail address: tujp@zju.edu.cn (J.P. Tu).

0378-7753/$ – see front matter © 2008 Elsevier B.V. All rights reserved.
doi:10.1016/j.jpowsour.2008.01.026

container and washed with distilled water several times, finally dried at 90 °C for 5 h. The microstructure and morphology of the as-prepared powder were characterized by powder X-ray diffraction (XRD, Rigaku D/max-rA diffractometer with Cu Kα radiation, λ = 1.5406 Å), a transmission electron microscope (TEM, JEM-2010) and scanning electron microscope (SEM, FEI SIRION JY/T010-1996).

2.2. Preparation of electrodes and test cells

The as-prepared ZnO active material, binders (PTFE, CMC and PVA), conductive acetylene carbon black and distilled water were mixed enough to make a homogeneous paste with adequate rheological properties. Then the paste was smeared into a foam nickel substrate (2 cm × 2 cm) to fabricate the Zn electrode. Afterwards, the pasted electrodes were dried at 70 °C and pressed at a pressure of 30 MPa. For comparison, a similar anode with conventional ZnO (bought from Xiaoshan Chemical Regent Factory, Hangzhou, China) was also fabricated according to the same process. A pasted nickel hydroxide (β-$Ni(OH)_2$) electrode served as the cathode. The ratio of designed capacity for the β-$Ni(OH)_2$ cathode and ZnO anode was about 3:1, so the capacity obtained in this present work just reflected the performance of ZnO electrode. A solution of 4 M KOH, 1.6 M K_2BO_3, 0.9 M KF and 0.1 M LiOH, saturated with ZnO, was used as the electrolyte, and a polyolefin microporous membrane as separator. The ZnO anode and β-$Ni(OH)_2$ cathode were assembled into a cell.

2.3. Electrochemical tests

The galvanostatic charge–discharge tests were conducted on a BS9300 Battery Program-control Test System at room temperature. The cells were charged at 0.2 C for 5 h, and then discharged at 0.2 C down to 1.2 V cut-off. The anodes after the charge–discharge tests were washed repeatedly in distilled water, rinsed with ethanol and air-dried, then examined using SEM.

Cyclic voltammogram (CV) measurements were performed on a CHI640B electrochemical workstation at room temperature with a scanning rate of 0.1 mV s^{-1}, shifting from −0.4 V to −1.55 V. A three-electrode cell assembly was used with a β-$Ni(OH)_2$ electrode as the counter electrode, a ZnO electrode as the working electrode and a Hg/HgO electrode as the reference electrode. The electrolyte was ZnO-saturated 6 M KOH solution.

3. Results and discussion

Fig. 1 shows the XRD pattern of the product prepared by the hydrothermal synthesis method. All the diffraction peaks can be indexed to wurtzite ZnO, and no other impurity peaks are observed. The pattern shows very sharp peaks, indicating that the ZnO nanoplates have good crystallization. The as-prepared ZnO product was further examined by SEM and TEM. From Fig. 2a, it can be seen that the as-prepared ZnO has irregular tetragonal plate-like morphology, the dimension of plate-like ZnO ranges from 200 to 500 nm and the average thickness of

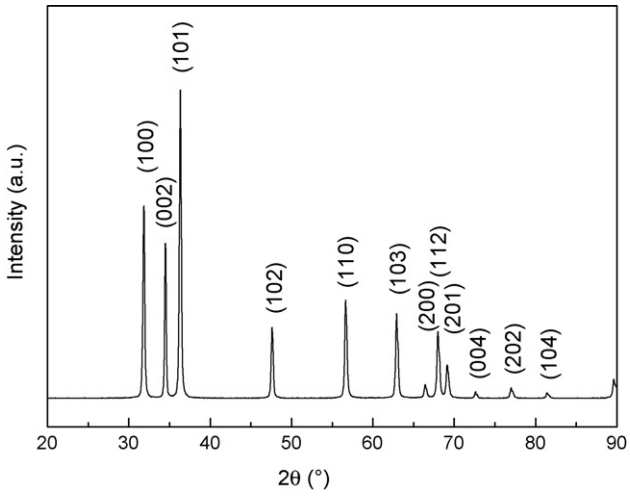

Fig. 1. XRD pattern of ZnO nanoplates prepared by the hydrothermal synthesis method.

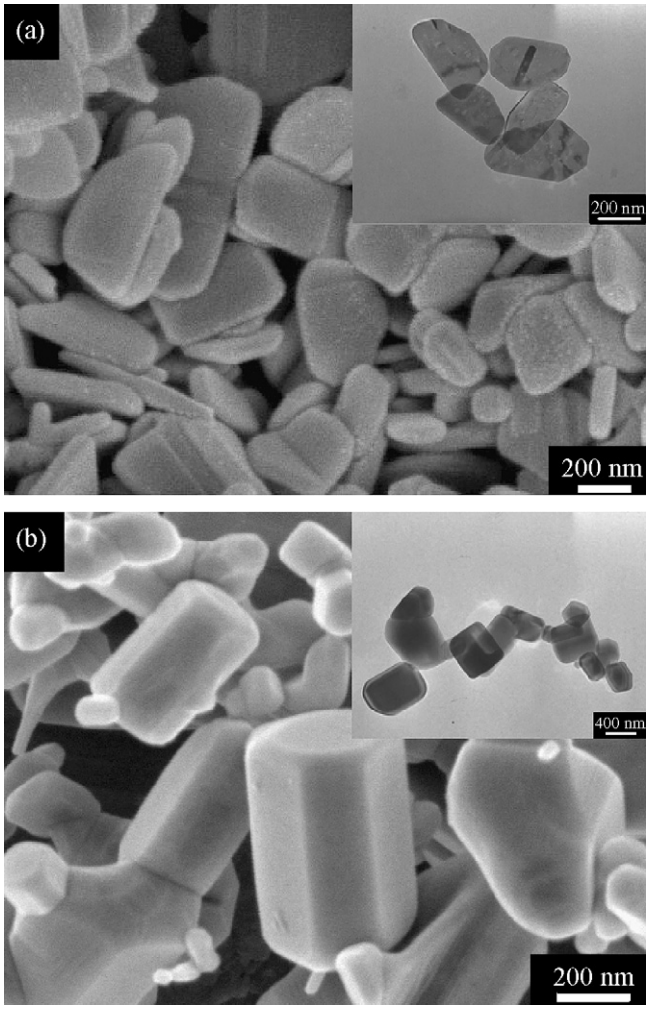

Fig. 2. (a) SEM micrographs of ZnO nanoplates prepared by the hydrothermal synthesis (inset: TEM micrographs of the ZnO nanoplates). (b) SEM micrographs of conventional ZnO (inset: TEM micrographs of conventional ZnO).

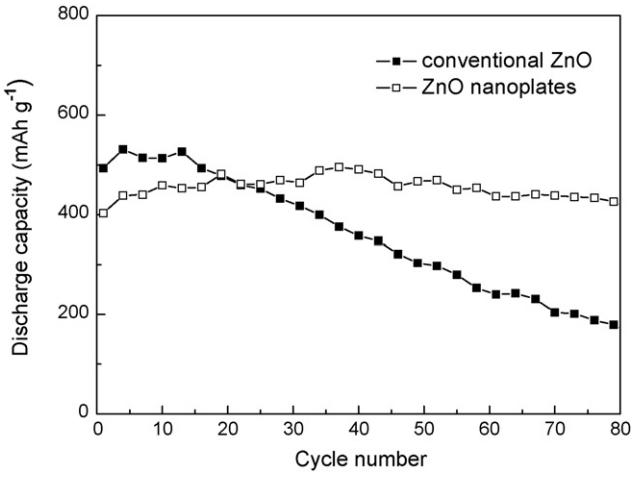

Fig. 3. Electrochemical cycle behavior of Ni/Zn cells with ZnO nanoplates and conventional ZnO as active materials.

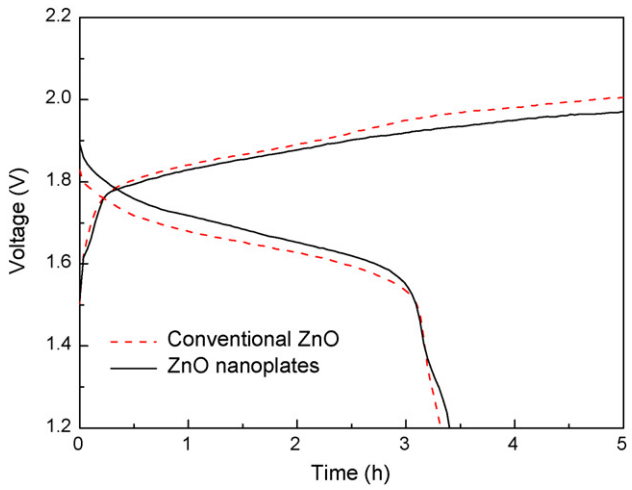

Fig. 4. Typical charge/discharge curves of Ni/Zn cells with ZnO nanoplates and conventional ZnO as active materials at the 20th cycle.

ZnO nanoplates is about 50 nm. For comparison, typical SEM and TEM micrographs of the conventional ZnO are shown in Fig. 2b. The conventional ZnO is a hexagonal prism elongated along the *c*-axis. The average diameter of prismatic ZnO is about 400 nm and its average length is about 500 nm.

The electrochemical cycle behavior of the pasted electrodes with conventional ZnO and ZnO nanoplates as active materials are illustrated in Fig. 3. The discharge capacity of conventional ZnO reaches the highest value 531 mAh g^{-1} at the fourth cycle. Nevertheless, it decays to 178 mAh g^{-1} rapidly after 80 cycles. The conventional ZnO exhibits a fading rate of 0.88%. Compared to the conventional ZnO, the discharge capacity delivered by ZnO nanoplates was more stable. Although the discharge capacity of ZnO nanoplates is only about 400 mAh g^{-1} in the initial several cycles and lower than that of conventional ZnO, the difference of discharge capacity rapidly decreases with the increase of cycling number. After the 18th cycle, the discharge capacity of ZnO nanoplates exceeds that of conventional ZnO and still remains 427 mAh g^{-1} until the 80th cycle. The fading rate of ZnO nanoplates is only 0.19%. The average discharge capacity of ZnO nanoplates is 455 mAh g^{-1}, which is higher than that of conventional ZnO.

The typical charge–discharge curves of Ni/Zn cells with ZnO nanoplates and conventional ZnO tested at the 20th cycle are displayed in Fig. 4. The Ni/Zn cells using ZnO nanoplates as anode materials show lower charge plateau voltage and higher discharge plateau voltage. The performance of the Ni/Zn cells is further assessed according to the change tendency of midpoint charge voltage and midpoint discharge voltage of the cells during cycling test. Fig. 5a shows the variation of midpoint charge voltage vs. cycle for the cells with ZnO nanoplates and conventional ZnO as active materials. Compared to the conventional ZnO, the midpoint charge voltage of ZnO nanoplates is obviously lower during most of the cycles, and the average charge plateau voltage of ZnO nanoplates is 100 mV lower than that of conventional ZnO. The decrease in midpoint charge voltage can result in an increase in charge efficiency and an enhancement of active material utilization in the anodes. Fig. 5b shows the

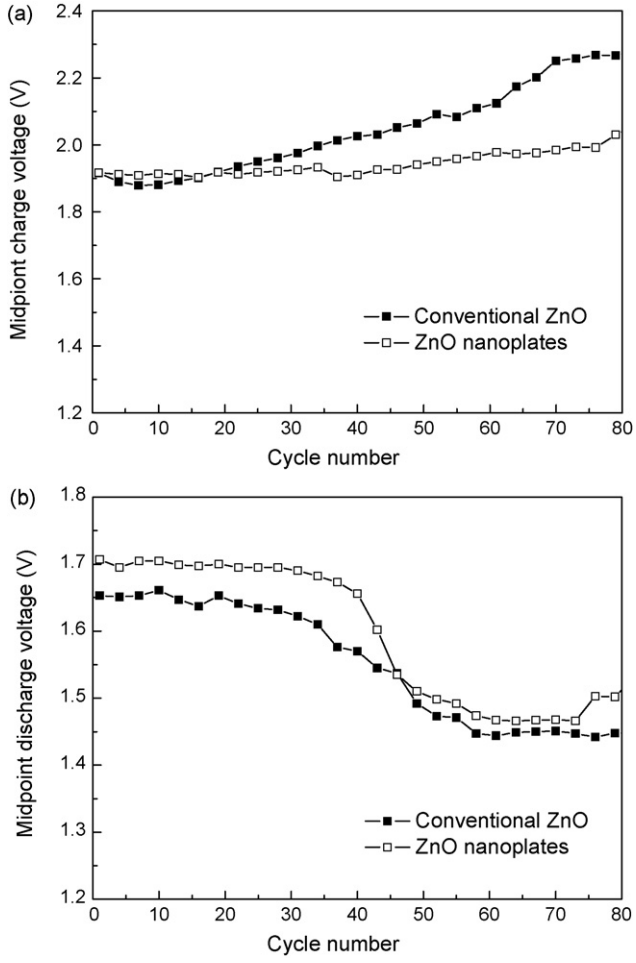

Fig. 5. (a) Variation of midpoint charge voltage vs. cycle for the cells with ZnO nanoplates and conventional ZnO as active materials, (b) variation of midpoint discharge voltage vs. cycle for the cells with ZnO nanoplates and conventional ZnO as active materials.

variation of midpoint discharge voltage vs. cycle for the cells with ZnO nanoplates and conventional ZnO as active materials. The midpoint discharge voltage is an important parameter for batteries. Higher midpoint discharge voltage associates with higher discharge potential, higher specific power and better performance in discharge. The average discharge plateau voltage of ZnO nanoplates is 40 mV higher than that of the conventional ZnO. In general, the ZnO nanoplates display better cell performance than the conventional ZnO.

The composition and structure of all tested cells are uniform, and the charge/discharge procedure is identical, thus the difference of electrochemical performance between the two kinds of cells is attributed to anode active material. In comparison with the conventional ZnO, the ZnO nanoplates have larger specific surface area. The increase in total surface area of active material decreases the resistance of the anodes, which results in a decrease in midpoint charge voltage and an increase in midpoint discharge voltage, according to

$$V = E_{\text{cathode}} - E_{\text{anode}} - I(R_{\Omega\text{anode}} + R_{\Omega\text{cathode}} + R_{\Omega\text{electrolyte}} + R_{\Omega\text{other}}) \text{ discharging mode} \quad (1)$$

$$V = E_{\text{cathode}} - E_{\text{anode}} + I(R_{\Omega\text{anode}} + R_{\Omega\text{cathode}} + R_{\Omega\text{electrolyte}} + R_{\Omega\text{other}}) \text{ discharging mode} \quad (2)$$

where E_{cathode} and E_{anode} are polarization potentials. This is consistent with the result in this work, which can be seen in Fig. 5. Besides, larger specific surface area can increase the effective reactive area of the active material and enhance its utilization. It indicates that the ZnO nanoplates are suitable for anode active material of Ni/Zn cells.

Fig. 6 shows the cyclic voltammogram curves of the ZnO nanoplates and the conventional ZnO in the solution of 6 M KOH saturated with ZnO on first scan. It can be seen that both of the current response lie between −1.0 V and −1.6 V. The curve is a beeline before −1.0 V. That is to say, no oxidative and reductive reaction occurred before −1.0 V. The cathode peak of ZnO nanoplates is much steeper than that of the conventional ZnO. The cathode peak is corresponding to reduce reaction of ZnO and charging process of secondary battery. This characteristic of cathode peak indicates that the ZnO nanoplates have rapid reduce reaction kinetics, and the charging process is more effective and rapid. The anode peak potential of the

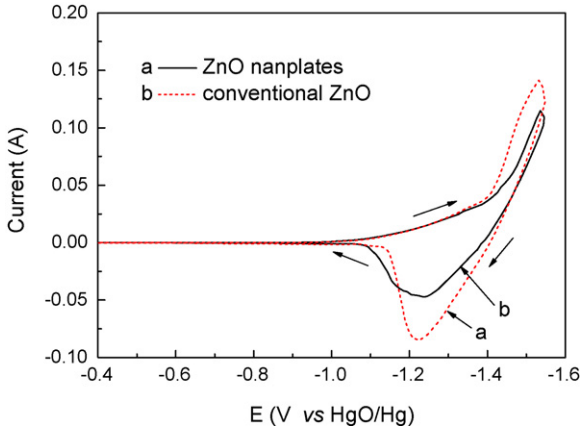

Fig. 6. Cyclic voltammogram curves of ZnO nanoplates and conventional ZnO at a scanning rate of 0.1 mV s^{-1} on first scan.

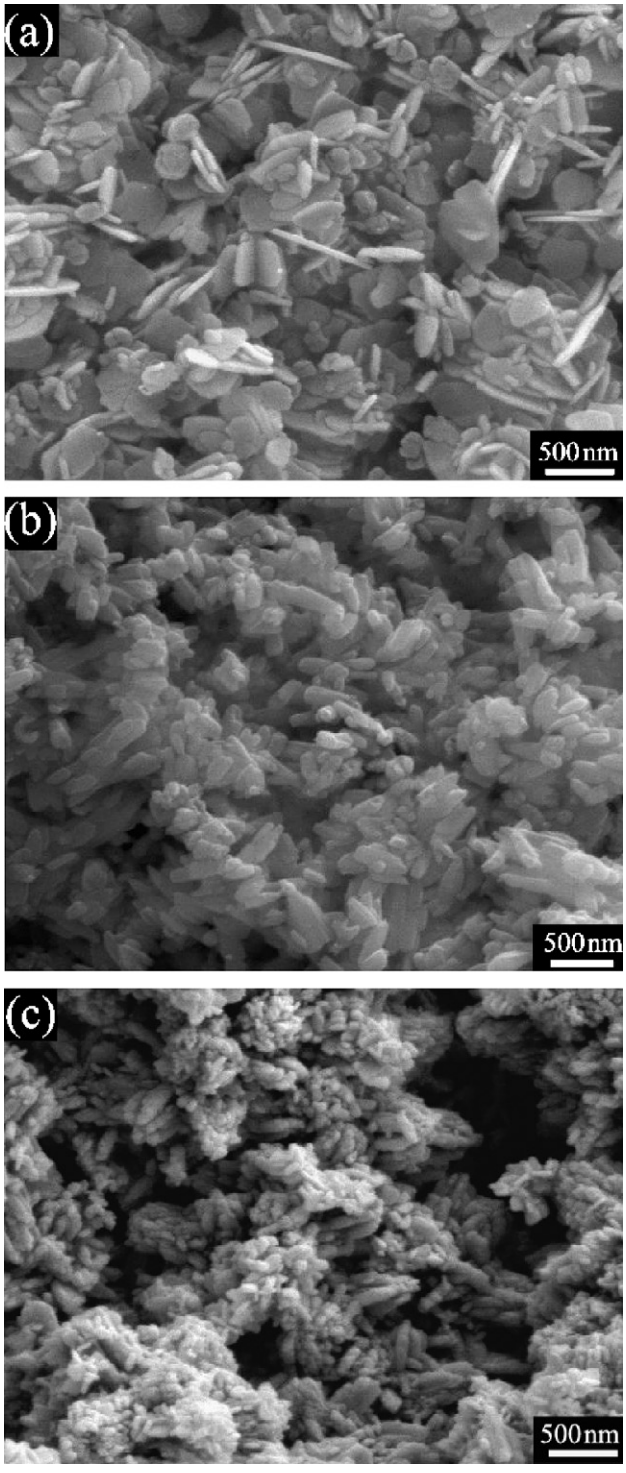

Fig. 7. Morphology evolution process of ZnO nanoplates: (a) as-prepared, (b) after 20 cycles, (c) after 67 cycles.

ZnO nanoplates and conventional ZnO is −1.22 V and −1.24 V, respectively. Obviously the anode peak potential of the ZnO nanoplates increases compared with the conventional ZnO. The anodic process is corresponding to the discharge process of the zinc electrode, hence the increase of the anode peak is in accord with the higher discharge voltage of the ZnO nanoplates. The area of anode peak of ZnO nanoplates is also larger than that of the conventional ZnO, which results from the higher electrochemical activity of ZnO nanoplates.

The charge process of the zinc electrode is controlled by liquid-side mass transfer. In general, there are three modes of liquid-side mass transfer: diffusion, migration, natural or forced convection. Mass-transport or diffusion could give rise to concentration polarization. The concentration polarization always plays a leading role in the cathode process and it determines the crystal morphology of electrodeposit. During charging, the concentration of the ions in the electrolyte near the surface of the zinc electrode becomes low and then it gives rise to concentration polarization. The zincate anions diffuse onto the protrusion on the surface of the electrode more easily than other position, therefore, the zincate anions may gradually build up and zinc dendrite forms. It is well known that ZnO is a hexagonal closed packed (hcp) structure and a polar crystal, whose polar axis is the *c*-axis. The thermodynamically stable crystal structure is wurtzite, which has a closest packed (0 0 0 1) crystal plane and a favorable stacking direction of ⟨0 0 0 1⟩. The growth velocities of ZnO crystal in different directions have been found to be: $V_{\langle 0\,0\,0\,1\rangle} > V_{\langle 0\,1\,\bar{1}\,0\rangle} V_{\langle 0\,0\,0\bar{1}\rangle}$. The maximal growth velocity is fixed in the ⟨0 0 0 1⟩ direction [17], and the electrodeposit will preferentially grow up in the ⟨0 0 0 1⟩ direction. Fig. 7 shows the morphology evolution process of the ZnO nanoplates during charge–discharge cycling. As shown in Fig. 7a, some of the nanoplates stand erect to the foam nickel substrate and others just incline to the substrate in the electrode before cycling. The arrangement of the nanoplates was not very tight and there was slightly interval between them, which could increase the effective reactive area and enhance the active material utilization. For the ZnO nanoplates, the rapidest growth direction determined by the crystal growth habit is vertical or inclined to the accelerated growth direction induced by concentration polarization which is aroused by liquid-side mass transfer. Therefore,

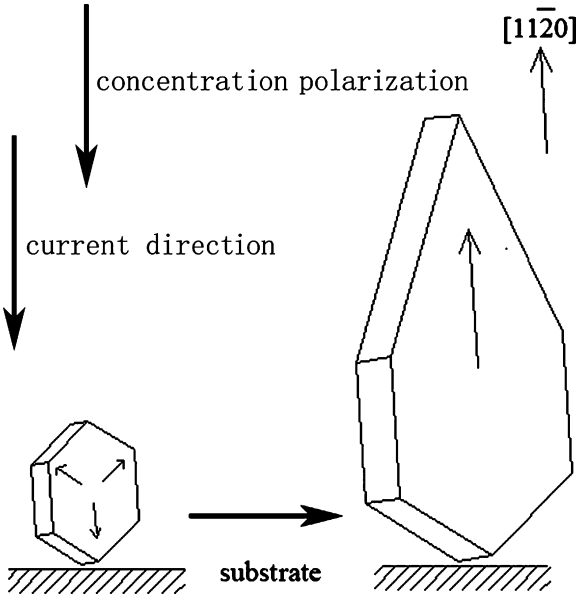

Fig. 8. Mechanism of suppressant effect of plate-like ZnO which stood erect to the substrate on the growth of zinc dendrite.

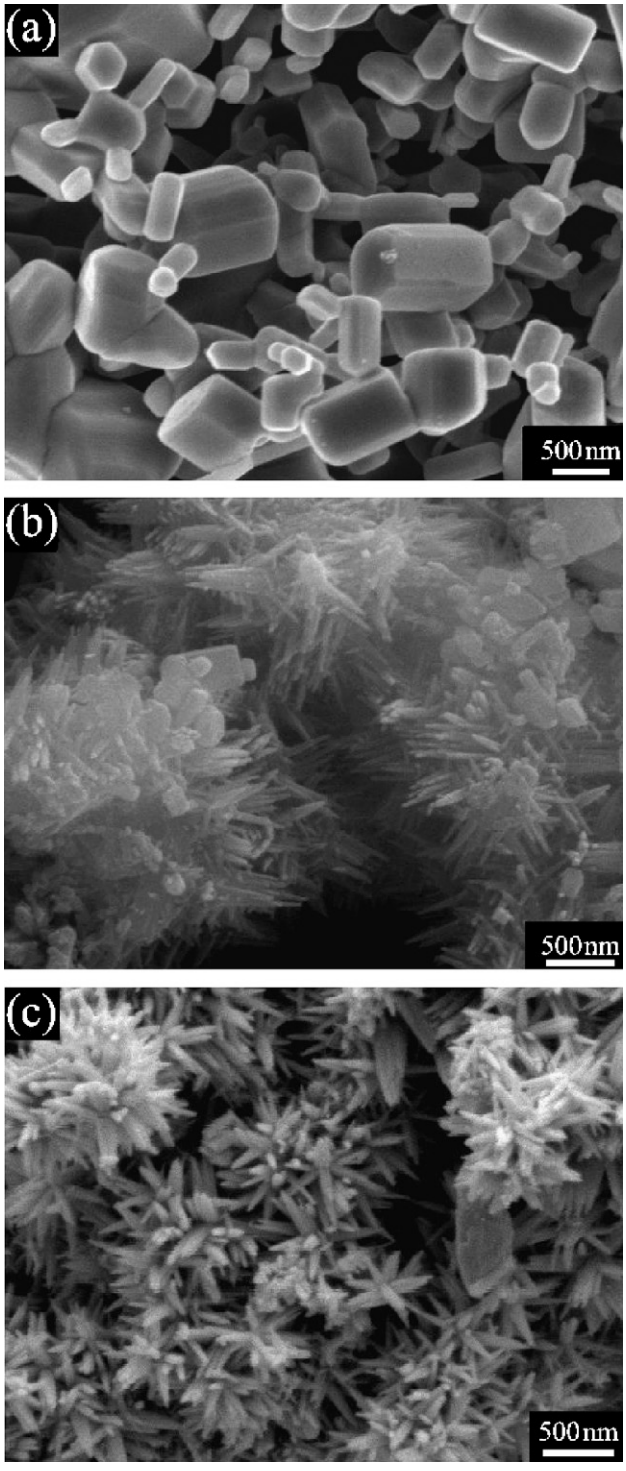

Fig. 9. Morphology evolution process of conventional ZnO: (a) raw material, (b) after 20 cycles, (c) after 67 cycles.

the concentration polarization can not give rise to the rapid growth in the ⟨0 0 0 1⟩ direction of the crystal and it will promote the fast growth in the ⟨1 1 $\bar{2}$ 0⟩ direction [14], as shown in Fig. 8. The fastest growth in the ⟨1 1 $\bar{2}$ 0⟩ direction and the rapidest growth direction determined by the crystal growth habit compete and mutually inhibit, hence the zinc dendrite is suppressed effectively. Fig. 7b shows the morphology of the zinc electrode after 20 charge–discharge cycles. The flaky structure gradually turned into spindle-like structure, the tip of the spindle was not spiculate and it seemed smoothly. The morphology characteristics could be attributed to the elongation of the ⟨1 1 $\bar{2}$ 0⟩ direction of the plate-like crystal. The average thickness of the nanoplates was about 50 nm and it was small, hence the surface activity of ZnO nanoplates was more intensive than that of the conventional ZnO, which made the epitaxial growth of ZnO nanoplates predominant [15]. Therefore the morphology of plate-like ZnO active material did not essentially change after 67 cycles, as shown in Fig. 7c. The morphology retention can stabilize the electrochemical performance of ZnO to a certain extent. On the other hand, the zinc electrode expanded during charge/discharge process, but the nanosized active materials had excellent plasticity and creep resistance [18]. At the same time, the volume change of them was small with the increase of cycle. Thus, for the ZnO nanoplates as active materials, the shape change of the zinc electrode could be restrained effectively and the discharge capacity of the cells would keep much more stable than that with the conventional ZnO as active material.

Fig. 9 shows the morphology evolution process of the conventional ZnO during charge–discharge cycling. From Fig. 9a, it can be seen that the structure of the conventional ZnO is hexagonal prism. After 20 charge/discharge cycles, the morphology of some prismatic ZnO did not essentially change but the others grew into acicular structure, as shown in Fig. 9b. With increasing the cycle, as shown in Fig. 9c, the prismatic ZnO almost disappeared and the tip of them turned into spiculate form, namely zinc dendrite came into being. The zinc dendrite might easily penetrate the separators and resulted in the interior short circuit, the shape of zinc electrode with the conventional ZnO as active material changed seriously, so the discharge capacity of the corresponding cells declined rapidly after 20 cycles, as shown in Fig. 3.

4. Conclusions

Compared to the conventional ZnO, ZnO nanoplates as anode materials for Ni/Zn cells show better discharge stability, lower midpoint charge voltage and higher midpoint discharge voltage. The reason for the maintenance of the discharge capacity should be attributed to the three factors: (1) The ZnO nanoplates which stood erect to the substrate grow rapidest in the ⟨1 1 $\bar{2}$ 0⟩ direction, the fastest growth in this direction and the rapidest growth direction determined by the crystal growth habit compete and inhibit mutually, hence the zinc dendrite is impeded effectively; (2) The morphology of ZnO nanoplates did not essentially change with increasing the cycle, and the morphology retention could stabilize electrochemical performance of the active material to a certain extent; (3) ZnO nanoplates had excellent plasticity and creep resistance. The volume of them change small with the increase of cycle, thus the shape change of the zinc electrode could be restrained enormously.

References

[1] R.E.F. Einerhand, W. Visscher, J. Electrochem. Soc. 138 (1991) 1.
[2] F.R. McLarnon, E.J. Cairns, J. Electrochem. Soc. 13 (1991) 645.
[3] M. Geng, D.O. Northwood, Int. J. Hydrogen Energy 28 (2003) 633.
[4] R. Shivkumar, G. Paruthimal Kalaignan, T. Vasudevan, J. Power Sources 75 (1998) 90.
[5] E. Frackowiak, J.M. Skrowronski, J. Power Sources 73 (1998) 175.
[6] D. Coates, E. Ferreira, A. Charkey, J. Power Sources 65 (1997) 109.
[7] J.X. Yu, H. Yang, X.P. Ai, X.M. Zhu, J. Power Sources 103 (2001) 93.
[8] Y.F. Yuan, J.P. Tu, H.M. Wu, C.Q. Zhang, S.F. Wang, X.B. Zhao, J. Power Sources 165 (2007) 905.
[9] J.L. Zhu, Y.H. Zhou, C.Q. Gao, J. Power Sources 72 (1998) 231.
[10] R. Renuka, S. Ramamurthy, K. Muralidharan, J. Power Sources 76 (1998) 197.
[11] T.C. Adler, F.R. McLarnon, J. Electrochem. Soc. 140 (1993) 289.
[12] J. Jindra, J. Power Sources 66 (1997) 15.
[13] J.L. Zhu, Y.H. Zhou, J. Power Sources 73 (1998) 266.
[14] Y.F. Yuan, J.P. Tu, H.M. Wu, D.Q. Shi, Nanotechnology 16 (2005) 803.
[15] Y.F. Yuan, J.P. Tu, H.M. Wu, B. Zhang, X.H. Huang, X.B. Zhao, J. Electrochem. Soc. 153 (2006) A1719.
[16] A. Pan, R. Yu, S. Xie, Z. Zhang, C. Jin, B. Zou, J. Cryst. Growth 282 (2005) 165.
[17] W.J. Li, E.W. Shi, W.Z. Zhong, Z.W. Yin, J. Cryst. Growth 203 (1999) 186.
[18] H.D. Li, C.L. Ma, The International Frontiers of Materials Science and Engineering, Science and Technology Press of Shangdong, Shangdong, 2003.